Title

Programmable RNA recognition and cleavage by CRISPR/Cas9

Journal

Nature, 516(7530)

ISSN

0028-0836

Authors

O'Connell, Mitchell R
Oakes, Benjamin L
Sternberg, Samuel H
et al.

Publication Date

2014-12-01

DOI

10.1038/nature13769

Peer reviewed

HHS Public Access

Author manuscript

Nature. Author manuscript; available in PMC 2015 June 11.

Published in final edited form as:

Nature. 2014 December 11; 516(7530): 263–266. doi:10.1038/nature13769.

Programmable RNA recognition and cleavage by CRISPR/Cas9

Mitchell R. O'Connell[1], **Benjamin L. Oakes**[1], **Samuel H. Sternberg**[2], **Alexandra East-Seletsky**[1], **Matias Kaplan**[3,†], and **Jennifer A. Doudna**[1,2,3,4]

[1]Department of Molecular and Cell Biology, University of California, Berkeley, California 94720, USA

[2]Department of Chemistry, University of California, Berkeley, California 94720, USA

[3]Howard Hughes Medical Institute, University of California, Berkeley, California 94720, USA

[4]Physical Biosciences Division, Lawrence Berkeley National Laboratory, Berkeley, California 94720, USA

Abstract

The CRISPR-associated protein Cas9 is an RNA-guided DNA endonuclease that uses RNA:DNA complementarity to identify target sites for sequence-specific doublestranded DNA (dsDNA) cleavage[1-5]. In its native context, Cas9 acts on DNA substrates exclusively because both binding and catalysis require recognition of a short DNA sequence, the protospacer adjacent motif (PAM), next to and on the strand opposite the 20-nucleotide target site in dsDNA[4-7]. Cas9 has proven to be a versatile tool for genome engineering and gene regulation in many cell types and organisms[8], but it has been thought to be incapable of targeting RNA[5]. Here we show that Cas9 binds with high affinity to single-stranded RNA (ssRNA) targets matching the Cas9-associated guide RNA sequence when the PAM is presented *in trans* as a separate DNA oligonucleotide. Furthermore, PAM-presenting oligonucleotides (PAMmers) stimulate site-specific endonucleolytic cleavage of ssRNA targets, similar to PAM-mediated stimulation of Cas9-catalyzed DNA cleavage[7]. Using specially designed PAMmers, Cas9 can be specifically directed to bind or cut RNA targets while avoiding corresponding DNA sequences, and we demonstrate that this strategy enables the isolation of a specific endogenous mRNA from cells. These results reveal a fundamental connection between PAM binding and substrate selection by Cas9, and highlight the utility of Cas9 for programmable and tagless transcript recognition.

CRISPR–Cas immune systems must discriminate between self and non-self to avoid an autoimmune response[9]. In type I and II systems, foreign DNA targets which contain adjacent PAM sequences are targeted for degradation, whereas potential targets in CRISPR loci of the host do not contain PAMs and are avoided by RNA-guided interference

---

Correspondence and requests for materials should be addressed to J.A.D. (doudna@berkeley.edu).

†Present address:Department of Agricultural and Biological Engineering, University of Florida, Gainesville, FL 32611, USA

M.R.O. and S.H.S. conceived the project. M.R.O., B.L.O., S.H.S., A.E.S and M.K. conducted experiments. All authors discussed the data, and M.R.O, S.H.S, B.L.O and J.A.D wrote the manuscript.

J.A.D., M.R.O, B.L.O, and S.H.S are inventors on a related patent.

complexes[3,5,6,10]. Single-molecule and bulk biochemical experiments showed that PAMs act both to recruit Cas9–guide RNA complexes (Cas9–gRNA) to potential target sites and to trigger nuclease domain activation[7]. Cas9 from *Streptococcus pyogenes* recognizes a 5'-NGG-3' PAM on the non-target (displaced) DNA strand[4,6], suggesting that PAM recognition may stimulate catalysis through allosteric regulation. Moreover, the HNH nuclease domain of Cas9, which mediates target strand cleavage[4,5], is homologous to other HNH domains that cleave RNA substrates[11,12]. Based on the observation that single-stranded DNA (ssDNA) targets can be activated for cleavage by a separate PAMmer oligonucleotide[7], and that similar HNH domains can cleave RNA, we wondered whether a similar strategy would enable Cas9 to cleave ssRNA targets in a programmable fashion (Fig. 1a).

Using *S. pyogenes* Cas9 and dual-guide RNAs (Methods), we performed *in vitro* cleavage experiments using a panel of RNA and DNA targets (Fig. 1b and Extended Table 1). Deoxyribonucleotide-comprised PAMmers specifically activated Cas9 to cleave ssRNA (Fig. 1c), an effect that required a 5'-NGG-3' or 5'-GG-3' PAM. RNA cleavage was not observed using ribonucleotide-based PAMmers, suggesting that Cas9 may recognize the local helical geometry and/or deoxyribose moieties within the PAM. Consistent with this idea, dsRNA targets were not cleavable, and RNA–DNA heteroduplexes could only be cleaved when the non-target strand was composed of deoxyribonucleotides. Interestingly, we found that Cas9 cleaved the ssRNA target strand between positions 4 and 5 of the base-paired guide RNA-target RNA hybrid (Fig. 1d), in contrast to the cleavage between positions 3 and 4 observed for dsDNA[3-5] likely due to subtle differences in substrate positioning. However, we did observe a significant reduction in the pseudo-first order cleavage rate constant of PAMmeractivated ssRNA as compared to ssDNA[7] (Extended Data Fig. 1).

We hypothesized that PAMmer nuclease activation would depend on the stability of the hybridized PAMmer–ssRNA duplex and tested this by varying PAMmer length. As expected, ssRNA cleavage was lost when the predicted melting temperature for the duplex decreased below the temperature used in our experiments (Fig. 1e). In addition, large molar excesses of di- or tri-deoxyribonucleotides in solution were poor activators of Cas9 cleavage (Extended Data Fig. 2). Collectively, these data demonstrate that hybrid substrate structures composed of ssRNA and deoxyribonucleotide-based PAMmers that anneal upstream of the RNA target sequence can be cleaved efficiently by RNA-guided Cas9.

We investigated the binding affinity of catalytically inactive (dCas9; D10A/H840A) dCas9–gRNA for ssRNA targets with and without PAMmers using a gel mobility shift assay. Intriguingly, while our previous results showed that ssDNA and PAMmer-activated ssDNA targets are bound with indistinguishable affinity[7], PAMmer-activated ssRNA targets were bound >500-fold tighter than ssRNA alone (Fig. 2a,b). A recent crystal structure of Cas9 bound to a ssDNA target revealed deoxyribose-specific van der Waals interactions between the protein and the DNA backbone[13], suggesting that energetic penalties associated with ssRNA binding must be attenuated by favorable compensatory binding interactions with the provided PAM. The equilibrium dissociation constant measured for a PAMmer–ssRNA substrate was within 5-fold of that for dsDNA (Fig. 2b), and this high-affinity interaction

again required a cognate deoxyribonucleotide-comprised 5'-GG-3' PAM (Fig. 2a). Tight binding also scaled with PAMmer length (Fig. 2c), consistent with the cleavage data presented above.

It was known that Cas9 possesses an intrinsic affinity for RNA, but sequence specificity of the interaction was not explored[5]. Thus, to verify the programmable nature of PAMmer-mediated ssRNA cleavage by Cas9–gRNA, we prepared three distinct guide RNAs (λ2, λ3, and λ4) and showed that their corresponding ssRNA targets could be efficiently cleaved using complementary PAMmers without any detectable cross-reactivity (Fig. 3a). This result indicates that complementary RNA–RNA base-pairing is critical in these reactions. Surprisingly, though, dCas9 programmed with the λ2 guide RNA bound all three PAMmer–ssRNA substrates with similar affinity (Fig. 3b). This observation suggests that high-affinity binding in this case may not require correct base-pairing between the guide RNA and the ssRNA target, particularly given the compensatory role of the PAMmer.

During dsDNA targeting by Cas9–gRNA, duplex melting proceeds directionally from the PAM and strictly requires formation of complementary RNA–DNA base-pairs to offset the energetic costs associated with dsDNA unwinding[7]. We therefore wondered whether binding specificity for ssRNA substrates would be recovered using PAMmers containing 5'-extensions that create a partially double-stranded target region requiring unwinding (Fig. 3c). Indeed, we found that use of a 5'-extended PAMmer enabled dCas9 bearing the λ2 guide sequence to bind sequence-selectively to the λ2 PAMmer–ssRNA target. The λ3 and λ4 PAMmer–ssRNA targets were not recognized (Fig. 3d and Extended Data Fig. 3), although we did observe a 10-fold reduction in overall ssRNA substrate binding affinity. By systematically varying the length of the 5' extension, we found that PAMmers containing 2–8 additional nucleotides upstream of the 5'-NGG-3' offer an optimal compromise between gains in binding specificity and concomitant losses in binding affinity and cleavage efficiency (Extended Data Fig. 4).

Next we investigated whether nuclease activation by PAMmers requires base-pairing between the 5'-NGG-3' and corresponding nucleotides on the ssRNA. Prior studies showed that DNA substrates containing a cognate PAM that is mismatched with the corresponding nucleotides on the target strand are cleaved as efficiently as a fully base-paired PAM[4]. Importantly, this could enable targeting of RNA while precluding binding or cleavage of corresponding genomic DNA sites lacking PAMs (Fig. 4a). To test this possibility, we first demonstrated that Cas9–gRNA cleaves PAMmer–ssRNA substrates regardless of whether or not the PAM is base-paired (Fig. 4b, c). When Cas9–RNA was incubated with both a PAMmer–ssRNA substrate and the corresponding dsDNA template containing a cognate PAM, both targets were cleaved. In contrast, when a dsDNA target lacking a PAM was incubated together with a PAMmer-ssRNA substrate bearing a mismatched 5'-NGG-3' PAM, Cas9–gRNA selectively targeted the ssRNA for cleavage (Fig. 4c). The same result was obtained using a mismatched PAMmer with a 5' extension (Fig. 4c), demonstrating that this general strategy enables the specific targeting of RNA transcripts while effectively eliminating any targeting of their corresponding dsDNA template loci.

We next explored whether Cas9-mediated RNA targeting could be applied for tagless transcript isolation from HeLa cells (Fig. 4d). The immobilization of Cas9 on a solid-phase resin is described in Methods (see also Extended Data Fig. 5). As a proof of concept, we first isolated *GAPDH* mRNA from HeLa total RNA using biotinylated dCas9, gRNAs and PAMmers (Extended Table 2) that target four non-PAM-adjacent sequences within exons 5–7 (Fig. 4e). We observed a substantial enrichment of *GAPDH* mRNA relative to a control *β-actin* mRNA by Northern blot analysis, but saw no enrichment using a non-targeting gRNA or dCas9 alone (Fig. 4f).

We then used this approach to isolate endogenous *GAPDH* transcripts from HeLa cell lysate under physiological conditions. In initial experiments, we found that Cas9–gRNA captured two *GAPDH*-specific RNA fragments rather than the full-length mRNA (Fig. 4g). Based on the sizes of these bands, we hypothesized that RNA:DNA heteroduplexes formed between the mRNA and PAMmer were cleaved by cellular RNase H. Previous studies have shown that modified DNA oligonucleotides can abrogate RNase H activity[14], and therefore we investigated whether Cas9 would tolerate chemical modifications to the PAMmer. We found that a wide range of modifications (locked nucleic acids, 2'-OMe and 2'-F ribose moieties) still enabled PAMmer-mediated nuclease activation (Extended Data Fig. 6). Importantly, by varying the pattern of 2'-OMe modifications in the PAMmer, we could completely eliminate RNase H-mediated cleavage during the pull-down and successfully isolate intact *GAPDH* mRNA (Fig. 4g,h). Interestingly, we consistently observed specific isolation of *GAPDH* mRNA in the absence of any PAMmer, albeit with lower efficiency, suggesting that Cas9–gRNA can bind to *GAPDH* mRNA through direct RNA:RNA hybridization (Fig. 4f,g and Extended Data Fig. 7). These experiments demonstrate that RNA-guided Cas9 can be used to purify endogenous untagged RNA transcripts. In contrast to current oligonucleotide-mediated RNA-capture methods, this approach works well under physiological salt conditions and does not require crosslinking or large sets of biotinylated probes[15-17].

Here we have demonstrated the ability to re-direct the dsDNA targeting capability of CRISPR/Cas9 for RNA-guided ssRNA binding and/or cleavage (RCas9). Programmable RNA recognition and cleavage has the potential to transform the study of RNA function much as site-specific DNA targeting is changing the landscape of genetic and genomic research[8] (Extended Data Fig. 8). Although certain engineered proteins such as PPR proteins and Pumilio/FBF (PUF) repeats show promise as platforms for sequence-specific RNA targeting[18- 22], these strategies require re-designing the protein for every new RNA sequence of interest. While RNA interference has proven useful for manipulating gene regulation in certain organisms[23], there has been a strong motivation to develop orthogonal nucleic acid-based RNA recognition systems, such as the CRISPR/Cas Type III-B Cmr complex[24-28] and the atypical Cas9 from *Francisella novicida*[29,30]. In contrast to these systems, the molecular basis for RNA recognition by RCas9 is now clear and requires only the design and synthesis of a matching gRNA and complementary PAMmer. The ability to recognize endogenous RNAs within complex mixtures with high affinity and in a programmable manner paves the way for direct transcript detection, analysis and manipulation without the need for genetically encoded affinity tags.

METHODS

Cas9 and nucleic acid preparation

Wild-type Cas9 and catalytically inactive dCas9 (D10A/H840A) from *S. pyogenes* were purified as previously described[4]. crRNAs (42 nt) were either ordered synthetically (Integrated DNA Technologies) or transcribed *in vitro* with T7 polymerase using single-stranded DNA templates, as described[31]. tracrRNA was transcribed *in vitro* and contained nucleotides 15–87 following the numbering scheme used previously[4]. λ-targeting sgRNAs were *in vitro* transcribed from linearized plasmids and contain full-length crRNA and tracrRNA connected via a GAAA tetraloop insertion. *GAPDH* mRNA-targeting sgRNAs were *in vitro* transcribed from dsDNA PCR products based on an optimized sgRNA design[32]. Target ssRNAs (55–56 nt) were *in vitro* transcribed using single-stranded DNA templates. Sequences of all nucleic acid substrates used in this study can be found in Extended Data Tables 1 & 2.

All RNAs were purified using 10–15% denaturing polyacrylamide gel electrophoresis (PAGE). crRNA–tracrRNA duplexes were prepared by mixing equimolar concentrations of each RNA in hybridization buffer (20 mM Tris-HCl, pH 7.5, 100 mM KCl, 5 mM $MgCl_2$), heating to 95 °C for 30 s and slow cooling. Fully double-stranded DNA/RNA substrates (substrates 1, 8–10 in Fig. 1 and substrates 1–2 in Fig. 4) were prepared by mixing equimolar concentrations of each nucleic acid strand in hybridization buffer, heating to 95 °C for 30 s, and slow cooling. RNA, DNA, and chemically modified PAMmers were synthesized commercially (Intergrated DNA Technologies). DNA and RNA substrates were 5'-radiolabeled using [γ-^{32}P]-ATP (PerkinElmer) and T4 polynucleotide kinase (New England Biolabs). dsDNA and dsRNA substrates (Fig. 1c, 4c) were 5'-radiolabeled on both strands, whereas only the target ssRNA was 5'-radiolabeled in other experiments.

Cleavage assays

Cas9–gRNA complexes were reconstituted before cleavage experiments by incubating Cas9 and the crRNA–tracrRNA duplex for 10 min at 37 °C in reaction buffer (20 mM Tris-HCl, pH 7.5, 75 mM KCl, 5 mM $MgCl^2$, 1 mM dithiothreitol (DTT), 5% glycerol). Cleavage reactions were conducted at 37 °C and contained ~1 nM 5′-radiolabeled target substrate, 100 nM Cas9–RNA, and 100 nM PAMmer, where indicated. Aliquots were removed at each time point and quenched by the addition of RNA gel loading buffer (95% deionized formamide, 0.025% (w/v) bromophenol blue, 0.025% (w/v) xylene cyanol, 50 mM EDTA (pH 8.0), 0.025% (w/v) SDS). Samples were boiled for 10 min at 95 °C prior to being resolved by 12% denaturing PAGE. Reaction products were visualized by phosphorimaging and quantified with ImageQuant (GE Healthcare).

RNA cleavage site mapping

A hydrolysis ladder (OH^-) was obtained by incubating ~25 nM 5′-radiolabeled λ2 target ssRNA in hydrolysis buffer (25 mM CAPS (*N*-cyclohexyl-3- aminopropanesulfonic acid), pH 10.0, 0.25 mM EDTA) at 95 °C for 10 min, before quenching on ice. An RNase T1 ladder was obtained by incubating ~25 nM 5′-radiolabeled λ2 target ssRNA with 1 Unit RNase T1 (NEB) for 5 min at 37 °C in RNase T1 buffer (20 mM sodium citrate, pH 5.0, 1

mM EDTA, 2 M urea, 0.1 mg mL^{-1} yeast tRNA). The reaction was quenched by phenol/chloroform extraction before adding RNA gel loading buffer. All products were resolved by 15% denaturing PAGE.

Electrophoretic mobility shift assays

In order to avoid dissociation of the Cas9–gRNA complex at low concentrations during target ssRNA binding experiments, binding reactions contained a constant excess of dCas9 (300 nM), increasing concentrations of sgRNA, and 0.1–1 nM of target ssRNA. The reaction buffer was supplemented with 10 μg ml^{-1} heparin in order to avoid non-specific association of apo-dCas9 with target substrates[7]. Reactions were incubated at 37 °C for 45 min before being resolved by 8% native PAGE at 4 °C (0.5× TBE buffer with 5 mM $MgCl_2$). RNA and DNA were visualized by phosphorimaging, quantified with ImageQuant (GE Healthcare), and analyzed with Kaleidagraph (Synergy Software).

Cas9 Biotin Labeling

To ensure specific labeling at a single residue on Cas9, two naturally occurring cysteine residues were mutated to serine (C80S and C574S) and a cysteine point mutant was introduced at residue M1. To attach the biotin moiety, 10 μM WT Cas9 or dCas9 was reacted with a 50-fold molar excess of EZ-Link® Maleimide-PEG2-Biotin (Thermo Scientific) at 25 °C for 2 h. The reaction was quenched by the addition of 10 mM DTT, and unreacted Maleimide-PEG2-Biotin was removed using a Bio-Gel® P-6 column (Bio-Rad). Labeling was verified using a streptavidin bead binding assay, where 8.5 pmol of biotinylated Cas9 or non-biotinylated Cas9 was mixed with either 25 μL streptavidin-agarose (Pierce Avidin Agarose; Thermo Scientific) or 25 μL streptavidin magnetic beads (Dynabeads MyOne Streptavidin C1; Life Technologies). Samples were incubated in Cas9 reaction buffer at RT for 30 min, followed by three washes with Cas9 reaction buffer and elution in boiling SDS-PAGE loading buffer. Elutions were analysed using SDS-PAGE. Cas9 M1C biotinylation was also confirmed using mass spectroscopy performed in the QB3/Chemistry Mass Spectrometry Facility at UC Berkeley. Samples of intact Cas9 proteins were analyzed using an Agilent 1200 liquid chromatograph equipped with a Viva C8 (100 mm × 1.0 mm, 5 μm particles, Restek) analytical column and connected in-line with an LTQ Orbitrap XL mass spectrometer (Thermo Fisher Scientific). Mass spectra were recorded in the positive ion mode. Mass spectral deconvolution was performed using ProMass software (Novatia).

GAPDH mRNA pull-down

HeLa-S3 cell lysates were prepared as previously described[33]. Total RNA was isolated from HeLa-S3 cells using Trizol reagent according to the manufacturer's instructions (Life Technologies). Cas9–sgRNA complexes were reconstituted before pull-down experiments by incubating a two-fold molar excess of Cas9 with sgRNA for 10 min at 37 °C in reaction buffer. HeLa total RNA (40 μg) or HeLa lysate (~5×10^6 cells) was added to reaction buffer with 40 U RNasin (Promega), PAMmer (5 μM) and the biotin-dCas9 (50 nM):sgRNA (25 nM) in a total volume of 100 μL and incubated at 37 °C for 1 h. This mixture was then added to 25 μL magnetic streptavidin beads (Dynabeads MyOne Streptavidin C1; Life Technologies) pre-equilibrated in reaction buffer and agitated at 4 °C for 2 h. Beads were

then washed six times with 300 μL wash buffer (20 mM Tris-HCl, pH 7.5, 150 mM NaCl, 5mM $MgCl_2$, 0.1% Triton X-100, 5% glycerol, 1mM DTT, 10 μg ml^{-1} heparin). Immobilized RNA was eluted by heating beads at 70 °C in the presence of DEPC-treated water and a phenol/chloroform mixture. Eluates were then treated with an equal volume of glyoxal loading dye (Life Technologies) and heated at 50 °C for 1 h before separation via 1% BPTE agarose gel (30 mM Bis-Tris, 10 mM PIPES, 10 mM EDTA, pH 6.5). Northern blot transfers were carried out according to Chomczynski *et al*.[34]. Following transfer, membranes were crosslinked using UV radiation and incubated in pre-hybridization buffer (UltraHYB® Ultrasensitive Hybridization Buffer; Life Technologies) for 1 h at 46 °C prior to hybridization. Radioactive Northern probes were synthesized using random priming of *GAPDH* and *β-actin* partial cDNAs (for cDNA primers, see Extended Data Table 2) in the presence of [α-^{32}P]-dATP (PerkinElmer), using a Prime-It II Random Primer Labeling kit (Agilent Technologies). Hybridization was carried out for 3 h in pre-hybridization buffer at 46 °C followed by two washes with 2×SSC (300 mM NaCl, 30 mM trisodium citrate, pH 7, 0.5% (w/v) SDS) for 15 min at 46 °C. Membranes were imaged using a phosphorscreen.

Extended Data

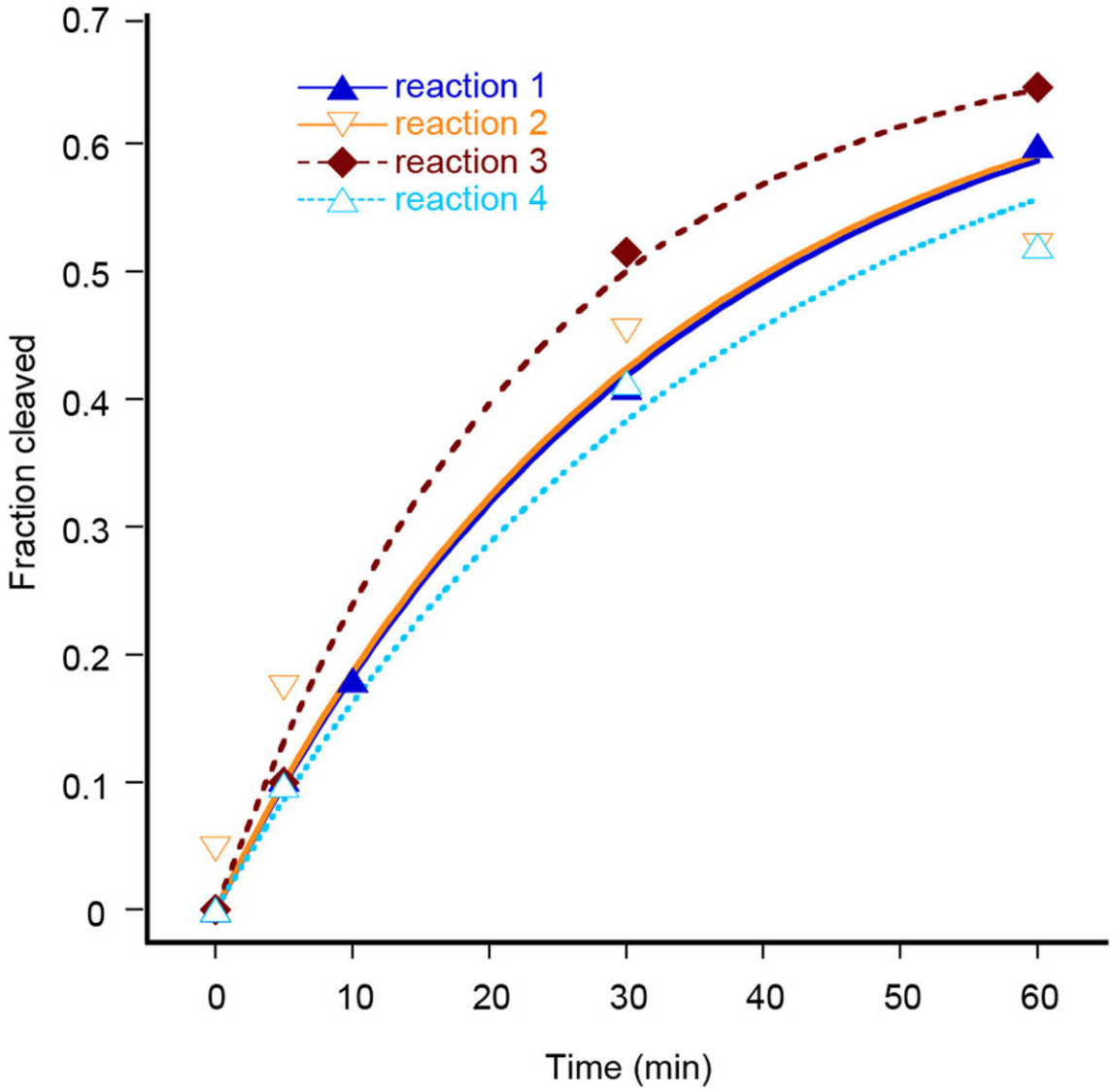

Extended Data Figure 1. Quantified data for cleavage of ssRNA by Cas9–gRNA in the presence of a 19-nt PAMmer

Cleavage assays were conducted as described in the Methods, and the quantified data were fit with single-exponential decays. Results from four independent experiments yielded an average apparent pseudo-first order cleavage rate constant of 0.032 ± 0.007 min^{-1}. This is slower than the rate constant determined previously for ssDNA in the presence of the same 19-nt PAMmer (7.3 ± 3.2 min^{-1})[7].

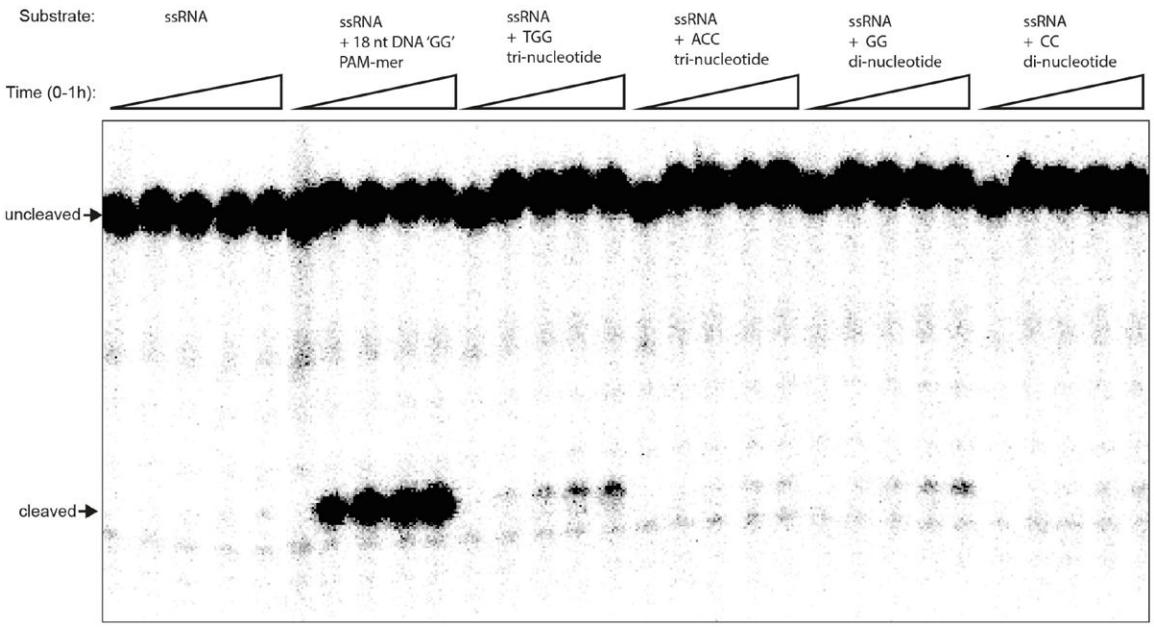

Extended Data Figure 2. RNA cleavage is marginally stimulated by di- and trideoxyribonucleotide PAMmers

Cleavage reactions contained ~1 nM 5′-radiolabelled target ssRNA and no PAMmer (left), 100 nM 18-nt PAMmer (second from left), or 1 mM of the indicated di- or tri-nucleotide (remaining lanes). Reaction products were resolved by 12% denaturing polyacrylamide gel electrophoresis (PAGE) and visualized by phosphorimaging.

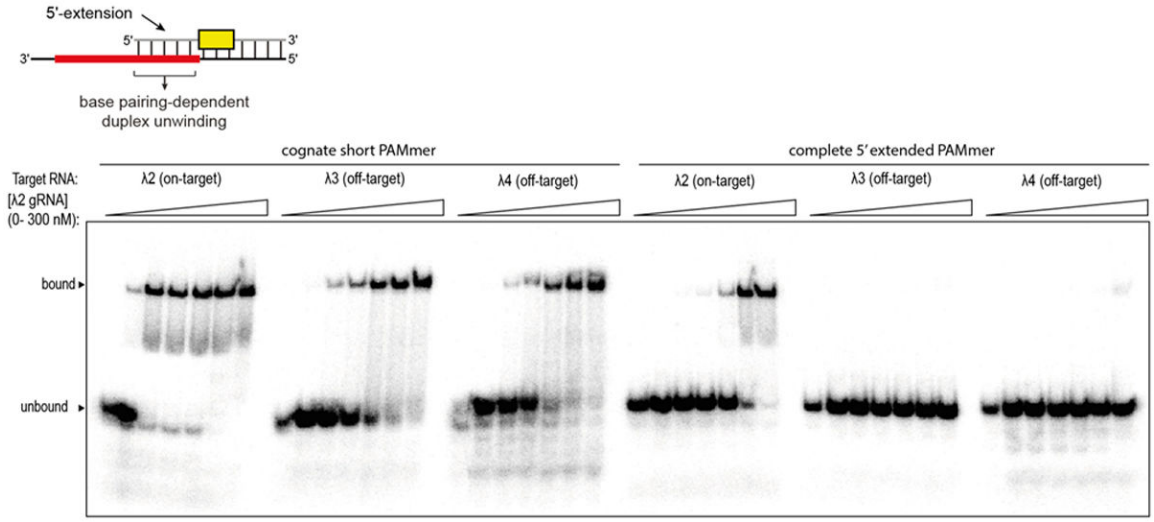

Extended Data Figure 3. Representative binding experiment demonstrating guide-specific ssRNA binding with 5′-extended PAMmers

Gel shift assays were conducted as described in the Methods. Binding reactions contained Cas9 programmed with λ2 gRNA and either λ2 (on-target), λ3 (off-target) or λ4 (off-target) ssRNA in the presence of short cognate PAMmers or cognate PAMmers with complete 5'-extensions, as indicated. The presence of a cognate 5'-extended PAM-mer abrogates off-

target binding. Three independent experiments were conducted to produce the data shown in Fig. 3b, d.

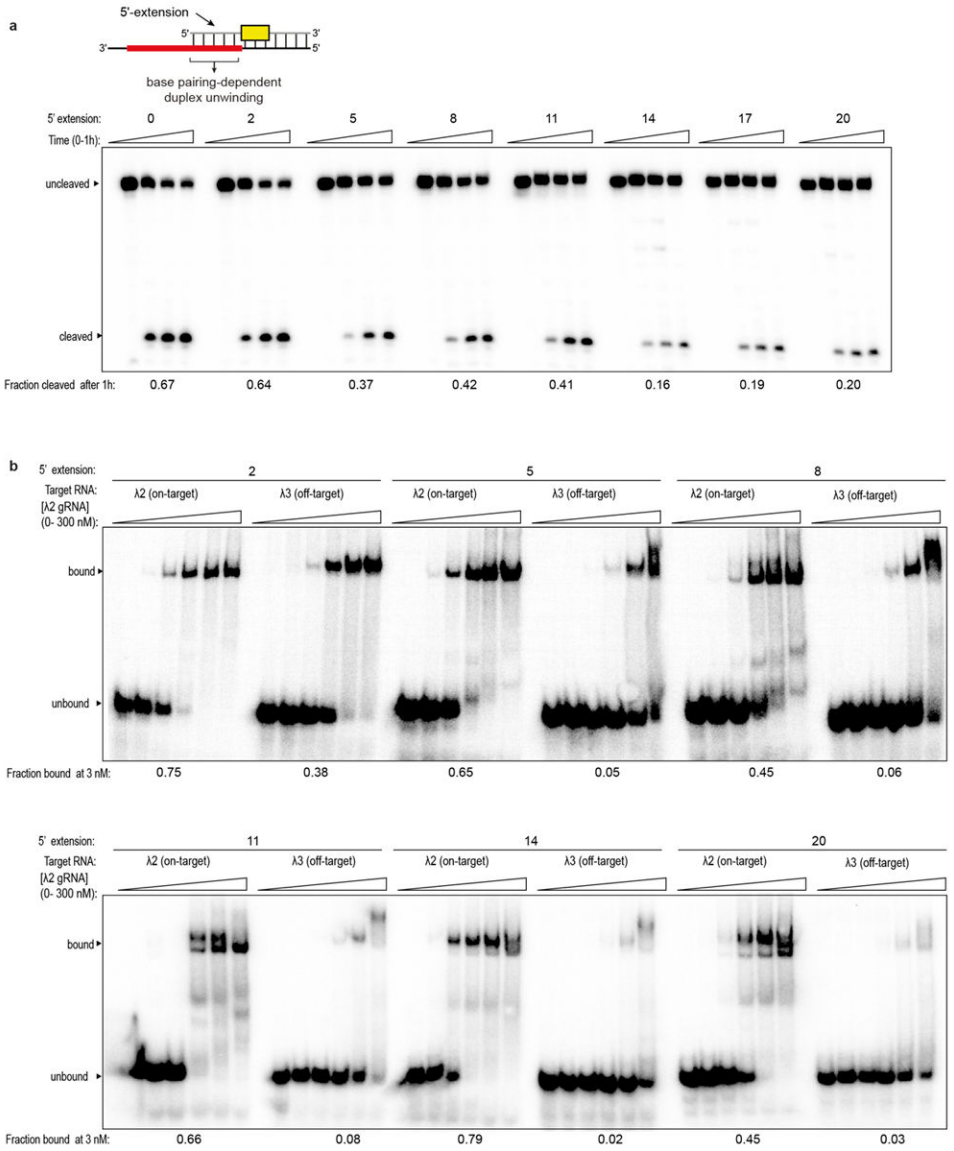

Extended Data Figure 4. Exploration of RNA cleavage efficiencies and binding specificity using PAMmers with variable 5′-extensions

a, Cleavage assays were conducted as described in Methods. Reactions contained Cas9 programmed with λ2 gRNA and λ2 ssRNA target in the presence of PAMmers with 5'-extensions of variable length. The ssRNA cleavage efficiency decreases as the PAMmer extends further into the target region, as indicated by the fraction RNA cleaved after 1 h. **b**, Binding assays were conducted as described in the Methods, using mostly the same panel of 5'-extended PAMmers as in (a). Binding reactions contained Cas9 programmed with λ2 gRNA and either λ2 (on-target) or λ3 (off-target) ssRNA in the presence of cognate PAMmers with 5'-extensions of variable length. The binding specificity increases as the PAMmer extends further into the target region, as indicated by the fraction of λ3 (off-target)

ssRNA bound at 3 nM Cas9-gRNA. PAMmers with 5' extensions also cause a slight reduction in the relative binding affinity of λ2 (on-target) ssRNA.

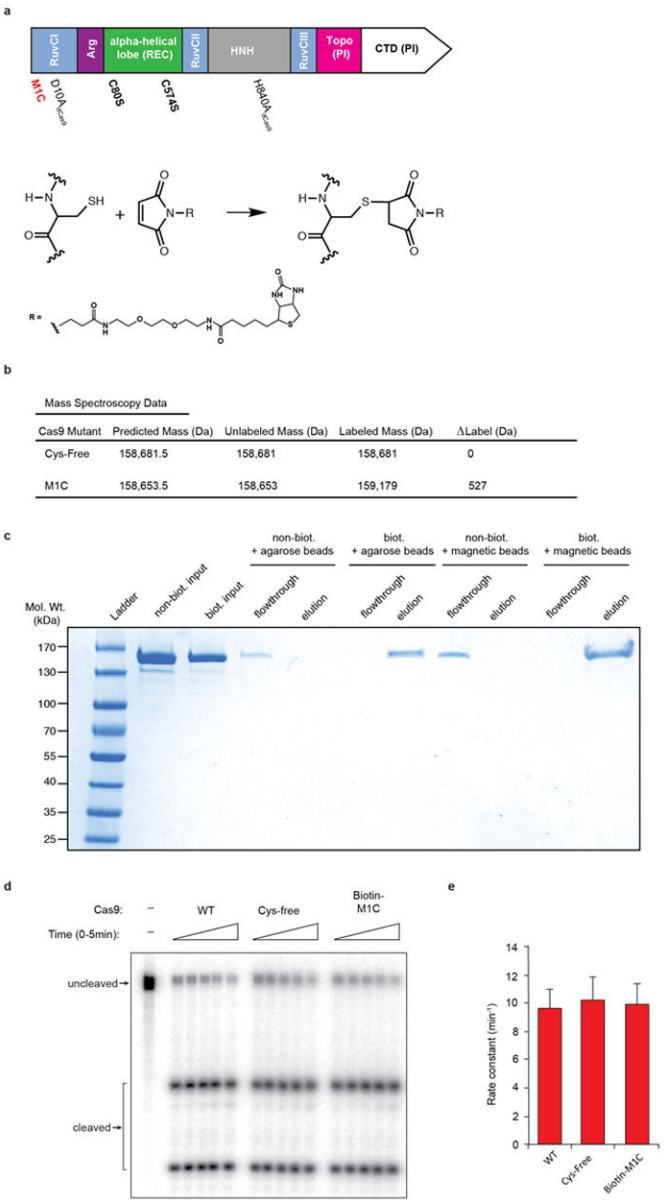

Extended Data Figure 5. Site-specific biotin labeling of Cas9

a, In order to introduce a single biotin moiety on Cas9, the solvent accessible, non-conserved N-terminal methionine was mutated to a cysteine (M1C; red text) and the naturally occurring cysteine residues were mutated to serine (C80S and C57S; bold text). This enabled cysteine-specific labeling with EZ-link® Maleimide-PEG2-biotin through an irreversible reaction between the reduced sulfhydryl group of the cysteine and the maleimide group present on the biotin label. dCas9 mutations are also indicated in the domain schematic. **b**, Mass spectrometry analysis of the Cas9 biotin labeling reaction confirmed that successful biotin labeling only occurs when the M1C mutation is present in the Cys-Free

background (C80S, C574S). The mass of the Maleimide-PEG2- biotin reagent is 525.6 Da. **c**, Streptavidin bead binding assay with biotinylated (biot.) or nonbiotinylated (non-biot.) Cas9 and streptavidin agarose or streptavidin magnetic beads. Cas9 only remains specifically bound to the beads after biotin labeling. **d**, Cleavage assays were conducted as described in the Methods and resolved by denaturing PAGE. Reactions contained 100 nM Cas9 programmed with λ2 gRNA and ~1 nM 5′-radiolabelled λ2 dsDNA target. **e**, Quantified cleavage data from triplicate experiments were fit with single-exponential decays to calculate the apparent pseudo-first order cleavage rate constants (average ± standard deviation). Both Cys-Free and Biotin-M1C Cas9 retain WT activity.

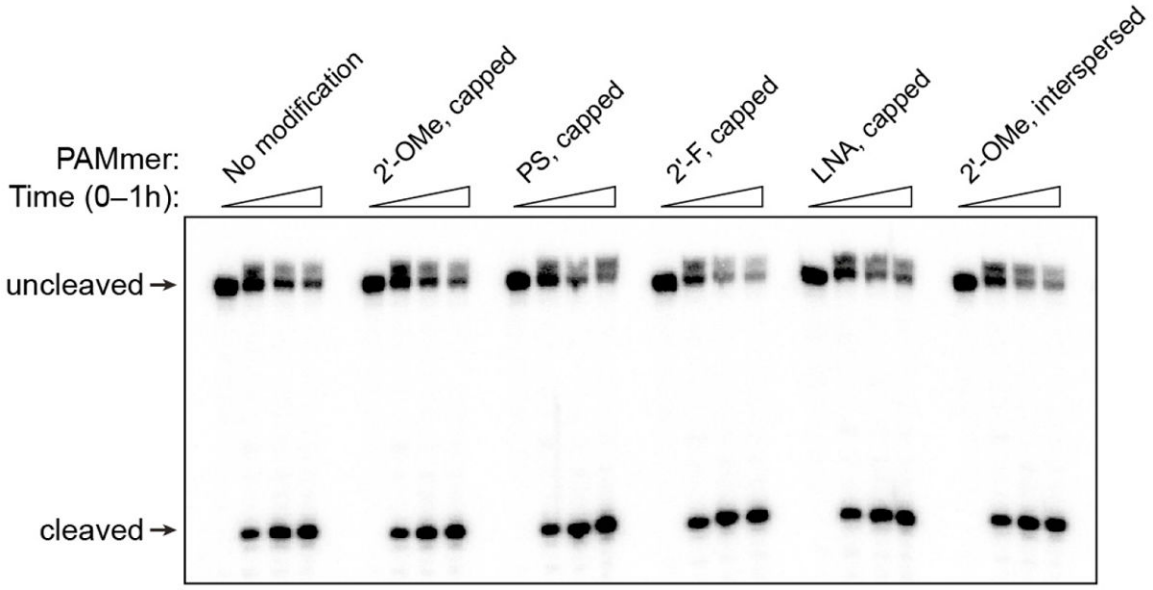

Extended Data Figure 6. RNA-guided Cas9 can utilize chemically modified PAMmers

19-nt PAMmer derivatives containing various chemical modifications on the 5' and 3' ends (capped) or interspersed still activate Cas9 for cleavage of ssRNA targets. These types of modification are often used to increase the *in vivo* half-life of short oligonucleotides by preventing exo- and endonuclease-mediated degradation. Cleavage assays were conducted as described in the Methods. PS, phosphorothioate bonds; LNA, locked nucleic acid.

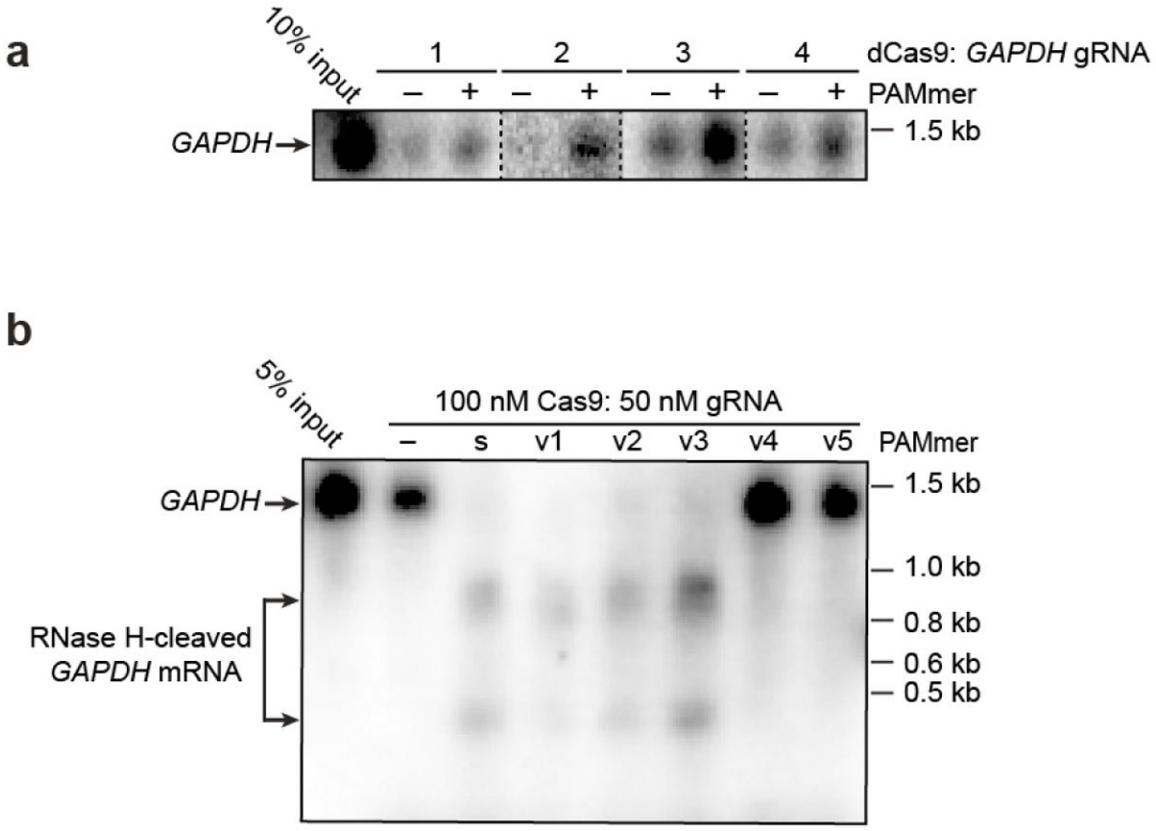

Extended Data Figure 7. Cas9 programmed with GAPDH-specific gRNAs can pull-down *GAPDH* mRNA in the absence of PAMmer

a, Northern blot showing that, in some cases, Cas9-gRNA is able to pull down detectable amounts of *GAPDH* mRNA from total RNA without requiring a PAMmer. **a**, Northern blot showing that Cas9-gRNA 1 is also able to pull-down quantitative amounts of *GAPDH* mRNA from HeLa cell lysate without requiring a PAMmer. s: standard; v: 2'-OMe-modified PAMmers.

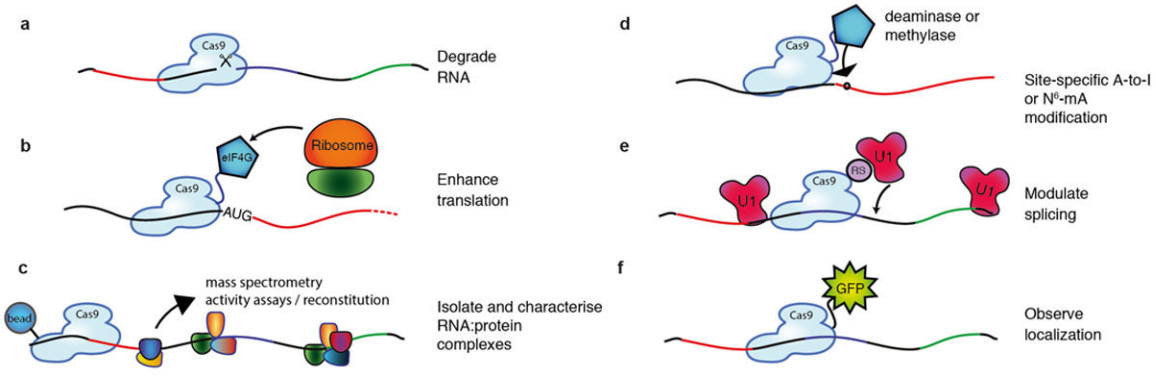

Extended Data Figure 8. Potential applications of RCas9 for untagged transcript analysis, detection, and manipulation

a, Catalytically-active RCas9 could be used to target and cleave RNA, particularly those for which RNAi-mediated repression/degradation is not possible. **b**, Tethering the eukaryotic

initiation factor eIF4G to a catalytically inactive dRCas9 targeted to the 5' untranslated region of an mRNA could drive translation. **c**, dRCas9 tethered to beads could be used to specificially isolate RNA or native RNA:protein complexes of interest from cells for downstream analysis or assays including identification of bound protein complexes, probing of RNA structure under native protein-bound conditions, and enrichment of rare transcripts for sequencing analysis. **d**, dRCas9 tethered to RNA deaminase or N^6-mA methylase domains could direct site-specific A-to-I editing or methylation or RNA, respectively. **e**, dRCas9 fused to a U1 recruitment domain (arginine- and serine-rich (RS) domain) could be programmed to recognize a splicing enhancer site and thereby promote the inclusion of a targeted exon. **f**, dRCas9 tethered to a fluorescent protein such as GFP could be used to observe RNA localization and transport in living cells.

Extended Data Table 1

λ oligonucleotide sequences

Description	Sequence *	Used in
Oligo for T7 promoter, in vitro transcription	5'-**TAATACGACTCACTATA**-3'	NA
λ2-targeting crRNA	5'-GUGAUAAGUGGAAUGCCAUGGUUUUAGAGCUAUGCUGUUUUG-3'	Fig. 1c-e, 3a, 4c-d, ED1-2, 4a
λ3-targeting crRNA	5'-CUGGUGAACUUCCGAUAGUGGUUUUAGAGCUAUGCUGUUUUG-3'	Fig. 3a
λ4-targeting crRNA	5'-CAGATATAGCCTGGTGGTTCGUUUUAGAGCUAUGCUGUUUUG-3'	Fig. 3a
ssDNA T7 template†, tracrRNA	5'-AAAAAGCACCGACTCGGTGCCACTTTTTCAAGTTGATAACGGACTAGCCTTATTTTAACTTGCTATGCTGT**CCTA TAGTGAGTCGTATTA**-3'	NA
tracrRNA (nt 15-87)	5'-GGACAGCAUAGCAAGUUAAAAUAAGGCUAGUCCGUUAUCAACUUGAAAAAGUGGCACCGAGUCGGUGCUUUUU-3'	Fig. 1c-e, 3a, 4c-d, ED1-2,4a
λ2-targeting sgRNA T7 template‡	5'-**TAATACGACTCACTATAGG**TGATAAGTGGAATGCCATGGTTTTAGAGCTATGCTGTTTTGGAAACAAAACAGCATA GCAAGTTAAAATAAGGCTAGTCCGTTATCAACTTGAAAAAGTGGCACCGAGTCGGTGCTTTTTTT-3'	NA
λ2-targeting sgRNA	5'-**GG**UGAUAAGUGGAAUGCCAUGGUUUUAGAGCUAUGCUGUUUUGGAAACAAAACAGCAUAGCAAGUUAAAAUAAGGC UAGUCCGUUAUCAACUUGAAAAAGUGGCACCGAGUCGGUGCUUUUUUU-3'	Fig 2, 3b,d, ED3, 4b
λ2 target dsDNA duplex	5'-GAGTGGAAGGATGCCAGTGATAAGTGGAATGCCATGTGGGCTGTCAAAATTGAGC-3' 3'-CTCACCTTCCTACGGTCACTATTCACCTTACGGTACACCCGACAGTTTTAACTCG-5'	Fig. 1c, 2a, 4c
λ2 ssDNA target strand (used to make heteroduplex DNA:RNA)	3'-CTCACCTTCCTACGGTCACTATTCACCTTACGGTACACCCGACAGTTTTAACTCG-5'	Fig. 1c, 2a
λ2 ssDNA non-target strand (used to make heteroduplex DNA:RNA)	5'-GAGTGGAAGGATGCCAGTGATAAGTGGAATGCCATGTGGGCTGTCAAAATTGAGC-3'	Fig 1c, 2a, 3d, ED3
λ2 ssRNA target strand T7 template	5'-GAGTGGAAGGATGCCAGTGATAAGTGGAATGCCATGTGGGCTGTCAAAATTGAGC**CTATAGTGAGTCGTATTA**-3'	NA
λ2 ssRNA target strand	3'-CUCACCUUCCUACGGUCACUAUUCACCUUACGGUACACCCGACAGUUUUAACUCGG-5'	Fig. 1c-e, 2, 3, 4, ED1-4
λ2 ssRNA non-target strand T7 template	5'-GCTCAATTTTGACAGCCCACATGGCATTCCACTTATCACTGGCATCCTTCCACTCC**TATAGTGAGTCGTATTA**-3'	NA
λ2 ssRNA non-target strand (used to make dsRNA)	5'-GGAGTGGAAGGATGCCAGTGATAAGTGGAATGCCATGTGGGCTGTCAAAATTGAGC-3'	Fig. 1c, 2a
19 nt λ2 DNA PAMmer	5'-TGGGCTGTCAAAATTGAGC-3'	Fig. 1c-e, 2, 3a-b, ED 1-4
18 nt λ2 "GG" DNA PAMmer	5'-GGGCTGTCAAAATTGAGC-3'	Fig. 1c, 2
19 nt λ2 DNA mutated PAMmer	5'-ACCGCTGTCAAAATTGAGC-3'	Fig. 1c, 2c
16 nt λ2 DNA "PAM-less" PAMmer	5'-GCTGTCAAAATTGAGC-3'	Fig. 1c, 2c
18 nt λ2 RNA PAMmer	5'-GGGCUGUCAAAAUUGAGC-3'	Fig. 1c, 2a
5 nt λ2 DNA PAMmer	5'-TGGGC-3'	Fig. 1e, 2c
10 nt λ2 DNA PAMmer	5'-TGGGCTGTCA-3'	Fig. 1e, 2c
15 nt λ2 DNA PAMmer	5'-TGGGCTGTCAAAATT-3'	Fig. 1e, 2c
λ3 ssRNA target strand T7 template	5'-AACGTGCTGCGGCTGGCTGGTGAACTTCCGATAGTGCGGGTGTTGAATGATTTCC**TATAGTGAGTCGTATTA**-3'	NA
λ3 ssRNA target strand	3'-UUGCACGACGCCGACCGACCACUUGAAGGCUAUCACGCCCACAACUUACUAAAGG-5'	Fig. 3a,b,d, ED3, 4b
λ4 ssRNA target strand T7 template	5'-TCACAACAATGAGTGGCAGATATAGCCTGGTGGTTCAGGCGGCGCATTTTTATTGC**TATAGTGAGTCGTATTA**-3'	NA
λ4 ssRNA target strand	3'-AGUGUUGUUACUCACCGUCUAUAUCGGACCACCAAGUCCGCCGCGUAAAAAUAACGG-5'	Fig. 3a,b,d, ED3
λ3 ssDNA non-target strand	5'-AACGTGCTGCGGCTGGCTGGTGAACTTCCGATAGTGCGGGTGTTGAATGATTTCC-3'	Fig. 3d, ED3
λ4 ssDNA non-target strand	5'-TCACAACAATGAGTGGCAGATATAGCCTGGTGGTTCAGGCGGCGCATTTTTATTG-3'	Fig. 3d, ED3
19 nt λ3 DNA PAMmer	5'-CGGGTGTTGAATGATTTCC-3'	Fig. 3a,b,d, ED3, 4
19 nt λ4 DNA PAMmer	5'-AGGCGGCGCATTTTTATTG-3'	Fig. 3a,b,d, ED3
21 nt λ2 5'-extended DNA PAMmer	5'-TGTGGGCTGTCAAAATTGAGC-3'	Fig. 4c, ED 4a,b
21 nt λ3 5'-extended DNA PAMmer	5'-TGCGGGTGTTGAATGATTTCC-3'	ED 4b
24 nt λ2 5'-extended DNA PAMmer	5'-CCATGTGGGCTGTCAAAATTGAGC-3'	ED 4a,b
24 nt λ3 5'-extended DNA PAMmer	5'-TAGTGCGGGTGTTGAATGATTTCC-3'	ED 4b
27 nt λ2 5'-extended DNA PAMmer	5'-ATGCCATGTGGGCTGTCAAAATTGAGC-3'	Fig. 4f,g, ED 4a,b
27 nt λ3 5'-extended DNA PAMmer	5'-CGATAGTGCGGGTGTTGAATGATTTCC-3'	ED 4b
30 nt λ2 5'-extended DNA PAMmer	5'-GGAATGCCATGTGGGCTGTCAAAATTGAGC-3'	ED 4a,b
30 nt λ3 5'-extended DNA PAMmer	5'-TTCCGATAGTGCGGGTGTTGAATGATTTCC-3'	ED 4b
33 nt λ2 5'-extended DNA PAMmer	5'-AGTGGAATGCCATGTGGGCTGTCAAAATTGAGC-3'	ED 4a,4b
33 nt λ3 5'-extended DNA PAMmer	5'-AACTTCCGATAGTGCGGGTGTTGAATGATTTCC-3'	ED 4b
36 nt λ2 5'-extended DNA PAMmer	5'-ATAAGTGGAATGCCATGTGGGCTGTCAAAATTGAGC-3'	ED 4a
39 nt λ2 5'-extended DNA PAMmer	5'-GTGATAAGTGGAATGCCATGTGGGCTGTCAAAATTGAGC-3'	ED 4a,4b
39 nt λ3 5'-extended DNA PAMmer	5'-CTGGTGAACTTCCGATAGTGCGGGTGTTGAATGATTTCC-3'	Fig. 4b
non-PAM λ2 dsDNA	5'-GAGTGGAAGGATGCCAGTGATAAGTGGAATGCCATGACCGCTGTCAAAATTGAGC-3' 3'-CTCACCTTCCTACGGTCACTATTCACCTTACGGTACTGGCGACAGTTTTAACTCG-5'	Fig. 4c
non-PAM λ2 ssRNA target strand T7 template	5'-GAGTGGAAGGATGCCAGTGATAAGTGGAATGCCATGACCGCTGTCAAAATTGAGC**CTATAGTGAGTCGTATTA**-3'	NA
non-PAM λ2 ssRNA target strand	3'-CUCACCUUCCUACGGUCACUAUUCACCUUACGGUACTGGCGACAGUUUUAACUCGG-5'	Fig. 4c
λ2 2'OMe capped PAMmer§	5'-*UGGGCUGUCAAAAUUGAG*C-3'	ED 6
λ2 PS capped PAMmer§	5'-T*GGGCTGTCAAAATTGAG*C-3'	ED 6
λ2 2'F capped PAMmer§	5'-*UGGGCUGUCAAAAUUGAG*C-3'	ED 6
λ2 LNA capped PAMmer§	5'-+TGGGCTGTCAAAATTGAG*C-3'	ED 6
λ2 19 nt 2'OMe interspersed PAMmer§	5'-*UGGG*CUGUC*AAAAUU*GAG*C-3'	ED 6

* Guide crRNA sequences and complementary DNA target strand sequences are shown in red. PAM sites (5'-NGG-3') are highlighted in yellow on the non-target strand when adjacent to the target sequence or in the PAMmer oligonucleotides.

† The T7 promoter is indicated in **bold** (or reverse complement of), as well as 5' G or GG included in the ssRNA product by T7 polymerase.

NA, not applicable.

‡ sgRNA template obtained from pIDT, subsequently linearised by AflII for run-off transcription.

§ Positions of modifications depicted with asterisks preceding each modified nucleotide in each case (except for PS linkages which are depicted between bases)

PS: phosphorothioate bond
LNA: locked nucleic acid

Extended Data Table 2

Oligonucleotides used in the *GAPDH* mRNA pull-down experiment

Description	Sequence *	Used in
GAPDH-targeting sgRNA 1 T7 template†	5′-**TAATACGACTCACTATA**GGGGCAGAGATGATGACCCTGTTTAAGAGCTATGCTGGAAACAGCATAGCAAGTTTAAATAA GGCTAGTCCGTTATCAACTTGAAAAAGTGGCACCGAGTCGGTGCTTTTTTT-3′	NA
GAPDH-targeting sgRNA 1	5′-GGGGCAGAGATGATGACCCTGTTTAAGAGCTATGCTGGAAACAGCATAGCAAGTTTAAATAAGGCTAGTCCGTTATCAAC TTGAAAAAGTGGCACCGAGTCGGTGCTTTTTTT-3′	Fig. 4f,g, ED 7
GAPDH-targeting sgRNA 2 T7 template†	5′-**TAATACGACTCACTATAGG**CCAAAGTTGTCATGGATGACGTTTAAGAGCTATGCTGGAAACAGCATAGCAAGTTTAAAT AAGGCTAGTCCGTTATCAACTTGAAAAAGTGGCACCGAGTCGGTGCTTTTTTT-3′	NA
GAPDH-targeting sgRNA 2	5′-**GG**CCAAAGTTGTCATGGATGACGTTTAAGAGCTATGCTGGAAACAGCATAGCAAGTTTAAATAAGGCTAGTCCGTTATCA ACTTGAAAAAGTGGCACCGAGTCGGTGCTTTTTTT-3′	Fig. 4f, ED 7
GAPDH-targeting sgRNA 3 T7 template†	5′-**TAATACGACTCACTATAGG**CCAAAGTTGTCATGGATGACGTTTAAGAGCTATGCTGGAAACAGCATAGCAAGTTTAAAT AAGGCTAGTCCGTTATCAACTTGAAAAAGTGGCACCGAGTCGGTGCTTTTTTT-3′	NA
GAPDH-targeting sgRNA 3	5′-**GG**CCAAAGTTGTCATGGATGACGTTTAAGAGCTATGCTGGAAACAGCATAGCAAGTTTAAATAAGGCTAGTCCGTTATCA ACTTGAAAAAGTGGCACCGAGTCGGTGCTTTTTTT-3′	Fig. 4f, ED 7
GAPDH-targeting sgRNA 4 T7 template†	5′-**GG**ATGTCATCATATTTGGCAGGGTTTAAGAGCTATGCTGGAAACAGCATAGCAAGTTTAAATAAGGCTAGTCCGTTATCA ACTTGAAAAAGTGGCACCGAGTCGGTGCTTTTTTT-3′	NA
GAPDH-targeting sgRNA 4	5′-**TAATACGACTCACTATAGG**ATGTCATCATATTTGGCAGGGTTTAAGAGCTATGCTGGAAACAGCATAGCAAGTTTAAAT AAGGCTAGTCCGTTATCAACTTGAAAAAGTGGCACCGAGTCGGTGCTTTTTTT-3′	Fig. 4f, ED 7
GAPDH PAMmer 1	5′-ATGACCCT**TGG**GGCTCCCCCCTGCAAA-3′	Fig. 4f,g, ED 7
GAPDH PAMmer 2	5′-TGGATGAC**CGG**GGCCAGGGGTGCTAAG-3′	Fig. 4f, ED 7
GAPDH PAMmer 3	5′-TTGGCAGG**TGG**TTCTAGACGGCAGGTC-3′	Fig. 4f, ED 7
GAPDH PAMmer 4	5′-CCCCAGCG**TGG**AAGGTGGAGGAGTGGG-3′	Fig. 4f, ED 7
GAPDH PAMmer 1 2′OMe v1‡	5′-A*UGACC*CTAGG*GGCTC*CCCCC*UGCAA*A-3′	Fig. 4g, ED 7
GAPDH PAMmer 1 2′OMe v2‡	5′-*ATG*ACC*CU*AGG*GGC*UCC*CCC*CTG*CAA*A-3′	Fig. 4g, ED 7
GAPDH PAMmer 1 2′OMe v3‡	5′-*ATG*ACCC*UAGG*GGCT*CCCC*CCTG*CAA*A-3′	Fig. 4g, ED 7
GAPDH PAMmer 1 2′OMe v4‡	5′-*AT*GA*CC*CT*AGG*GG*CT*CC*CC*CC*UG*CA*AA-3′	Fig. 4g, ED 7
GAPDH PAMmer 1 2′OMe v5‡	5′-*AT*GA*CC*CT*AG*GG*GC*TC*CC*CC*CU*GC*AA*A-3′	Fig. 4g, ED 7
GAPDH cDNA primer Fwd	5′-CTCACTGTTCTCTCCCTCCGC-3′	Fig. 4g,f, ED7
GAPDH cDNA primer Rev	5′-AGGGGTCTACATGGCAACTG-3′	Fig. 4g,f, ED7
β-actin cDNA primer Fwd	5′-AGAAAATCTGGCACCACACC-3′	Fig. 4g,f, ED7
β-actin cDNA primer Rev	5′-GGAGTACTTGCGCTCAGGAG-3′	Fig. 4g,f, ED7

* Guide crRNA sequences and complementary DNA target strand sequences are shown in red. PAM sites (5'-NGG-3') are highlighted in yellow on the non-target strand when adjacent to the target sequence or in the PAMmer oligonucleotides.

† The T7 promoter is indicated in **bold** (or reverse complement of), as well as 5' G or GG included in the ssRNA product by T7 polymerase. sgRNAs for *GAPDH* were designed according to Chen, B. *et al*. Dynamic imaging of genomic loci in living human cells by an optimized CRISPR/Cas system. *Cell* **155**, 1479-1491 (2013).

NA, not applicable.

‡ Positions of 2'OMe modifications depicted with asterisks preceding each modified nucleotide in each.

Supplementary Material

Refer to Web version on PubMed Central for supplementary material.

Acknowledgments

We thank B. Staahl and K. Zhou for technical assistance, A. Iavarone for assistance with mass spectrometry measurements, Integrated DNA Technologies for the synthesis of DNA and RNA oligonucleotides, and members of the Doudna laboratory and J. Cate for helpful discussions and critical reading of the manuscript. S.H.S. acknowledges support from the National Science Foundation and National Defense Science & Engineering Graduate Research Fellowship programs. A.E.S and B.L.O acknowledge support from NIH NRSA trainee grants. Funding was provided NIH-funded Center for RNA Systems Biology (5P50GM102706-03). J.A.D. is an Investigator of the Howard Hughes Medical Institute.

References

1. Wiedenheft B, Sternberg SH, Doudna JA. RNA-guided genetic silencing systems in bacteria and archaea. Nature. 2012; 482:331–338. [PubMed: 22337052]
2. Barrangou R, et al. CRISPR provides acquired resistance against viruses in prokaryotes. Science. 2007; 315:1709–1712. [PubMed: 17379808]
3. Garneau JE, et al. The CRISPR/Cas bacterial immune system cleaves bacteriophage and plasmid DNA. Nature. 2010; 468:67–72. [PubMed: 21048762]
4. Jinek M, et al. A programmable dual-RNA-guided DNA endonuclease in adaptive bacterial immunity. Science. 2012; 337:816–821. [PubMed: 22745249]
5. Gasiunas G, Barrangou R, Horvath P, Siksnys V. Cas9-crRNA ribonucleoprotein complex mediates specific DNA cleavage for adaptive immunity in bacteria. Proc Natl Acad Sci U S A. 2012; 109:E2579–2586. [PubMed: 22949671]
6. Mojica FJM, Diez-Villasenor C, Garcia-Martinez J, Almendros C. Short motif sequences determine the targets of the prokaryotic CRISPR defence system. Microbiol. 2009; 155:733–740.
7. Sternberg SH, Redding S, Jinek M, Greene EC, Doudna JA. DNA interrogation by the CRISPR RNA-guided endonuclease Cas9. Nature. 2014; 507:62–67. [PubMed: 24476820]
8. Mali P, Esvelt KM, Church GM. Cas9 as a versatile tool for engineering biology. Nat Methods. 2013; 10:957–963. [PubMed: 24076990]
9. Marraffini LA, Sontheimer EJ. Self versus non-self discrimination during CRISPR RNA-directed immunity. Nature. 2010; 463:568–571. [PubMed: 20072129]
10. Sashital DG, Wiedenheft B, Doudna JA. Mechanism of Foreign DNA Selection in a Bacterial Adaptive Immune System. Mol Cell. 2012; 46:606–615. [PubMed: 22521690]
11. Pommer AJ, et al. Mechanism and cleavage specificity of the H-N-H endonuclease colicin E9. J Mol Biol. 2001; 314:735–749. [PubMed: 11733993]
12. Hsia KC, et al. DNA binding and degradation by the HNH protein ColE7. Structure. 2004; 12:205–214. [PubMed: 14962381]
13. Nishimasu H, et al. Crystal Structure of Cas9 in Complex with Guide RNA and Target DNA. Cell. 2014
14. Wu HJ, Lima WF, Crooke ST. Properties of cloned and expressed human RNase H1. J Biol Chem. 1999; 274:28270–28278. [PubMed: 10497183]
15. Engreitz JM, et al. The Xist lncRNA Exploits Three-Dimensional Genome Architecture to Spread Across the X Chromosome. Science. 2013; 341
16. Chu C, Qu K, Zhong FL, Artandi SE, Chang HY. Genomic Maps of Long Noncoding RNA Occupancy Reveal Principles of RNA-Chromatin Interactions. Mol Cell. 2011; 44:667–678. [PubMed: 21963238]
17. Simon MD, et al. The genomic binding sites of a noncoding RNA. P Natl Acad Sci USA. 2011; 108:20497–20502.
18. Mackay JP, Font J, Segal DJ. The prospects for designer single-stranded RNA-binding proteins. Nature Struct Mol Biol. 2011; 18:256–261. [PubMed: 21358629]
19. Filipovska A, Rackham O. Designer RNA-binding proteins: New tools for manipulating the transcriptome. RNA Biol. 2011; 8:978–983. [PubMed: 21941129]

20. Wang Y, Wang Z, Tanaka Hall TM. Engineered proteins with Pumilio/fem-3 mRNA binding factor scaffold to manipulate RNA metabolism. FEBS J. 2013; 280:3755–3767. [PubMed: 23731364]
21. Yin P, et al. Structural basis for the modular recognition of single-stranded RNA by PPR proteins. Nature. 2013; 504:168–171. [PubMed: 24162847]
22. Yagi Y, Nakamura T, Small I. The potential for manipulating RNA with pentatricopeptide repeat proteins. Plant J. 2014; 78:772–782. [PubMed: 24471963]
23. Kim DH, Rossi JJ. RNAi mechanisms and applications. Biotechniques. 2008; 44:613–616. [PubMed: 18474035]
24. Hale CR, et al. RNA-Guided RNA Cleavage by a CRISPR RNA-Cas Protein Complex. Cell. 2009; 139:945–956. [PubMed: 19945378]
25. Hale CR, et al. Essential Features and Rational Design of CRISPR RNAs that Function with the Cas RAMP Module Complex to Cleave RNAs. Mol Cell. 2012; 45:292–302. [PubMed: 22227116]
26. Staals RHJ, et al. Structure and Activity of the RNA-Targeting Type III-B CRISPR-Cas Complex of Thermus thermophilus. Mol Cell. 2013; 52:135–145. [PubMed: 24119403]
27. Spilman M, et al. Structure of an RNA Silencing Complex of the CRISPR-Cas Immune System. Mol Cell. 2013; 52:146–152. [PubMed: 24119404]
28. Terns RM, Terns MP. CRISPR-based technologies: prokaryotic defense weapons repurposed. Trends Genet. 2014; 30:111–118. [PubMed: 24555991]
29. Sampson TR, Saroj SD, Llewellyn AC, Tzeng YL, Weiss DS. A CRISPR/Cas system mediates bacterial innate immune evasion and virulence. Nature. 2013; 501:262–262. [PubMed: 23925120]
30. Sampson TR, Weiss DS. Exploiting CRISPR/Cas systems for biotechnology. Bioessays. 2014; 36:34–38. [PubMed: 24323919]
31. Sternberg SH, Haurwitz RE, Doudna JA. Mechanism of substrate selection by a highly specific CRISPR endoribonuclease. RNA. 2012; 18:661–672. [PubMed: 22345129]
32. Chen B, et al. Dynamic imaging of genomic loci in living human cells by an optimized CRISPR/Cas system. Cell. 2013; 155:1479–1491. [PubMed: 24360272]
33. Lee HY, et al. RNA-protein analysis using a conditional CRISPR nuclease. Proc Natl Acad Sci USA. 2013; 110:5416–5421. [PubMed: 23493562]
34. Chomczynski P. One-Hour Downward Alkaline Capillary Transfer for Blotting of DNA and RNA. Anal Biochem. 1992; 201

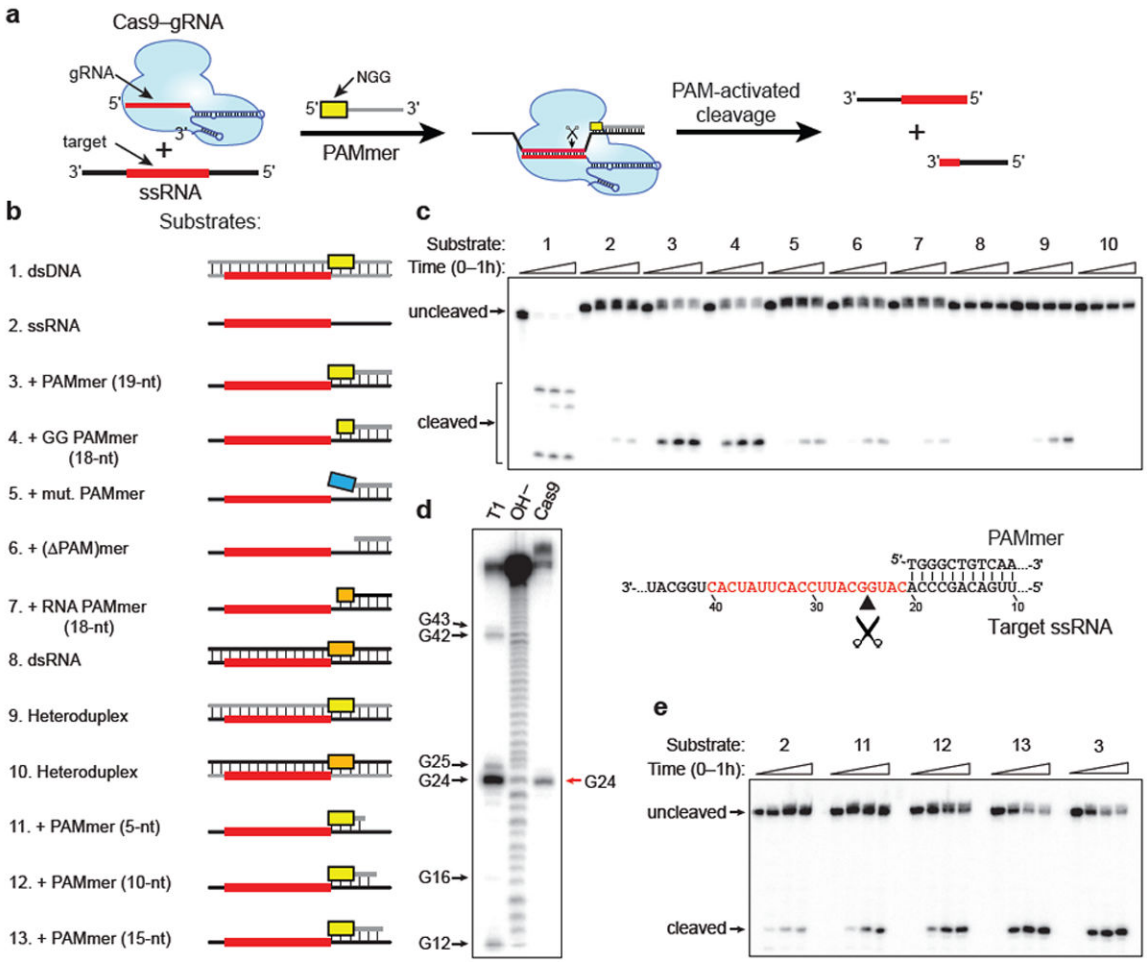

Figure 1. RNA-guided Cas9 cleaves ssRNA targets in the presence of a short PAM-presenting DNA oligonucleotide (PAMmer)

a, Schematic depicting the approach used to target ssRNA for programmable, sequence-specific cleavage. **b**, The panel of nucleic acid substrates examined in this study. Substrate elements are colored as follows: DNA (grey), RNA (black), guide RNA target sequence (red), DNA PAM (yellow), mutated DNA PAM (blue), RNA PAM (orange). **c**, Representative cleavage assay for 5'-radiolabeled nucleic acid substrates using Cas9–gRNA, numbered as in (**b**). **d**, Cas9–gRNA cleavage site mapping assay for substrate 3. T1 and OH^- denote RNase T1 and hydrolysis ladders, respectively; the sequence of the target ssRNA is shown at right. **e**, Representative ssRNA cleavage assay in the presence of PAMmers of increasing length, numbered as in (**b**).

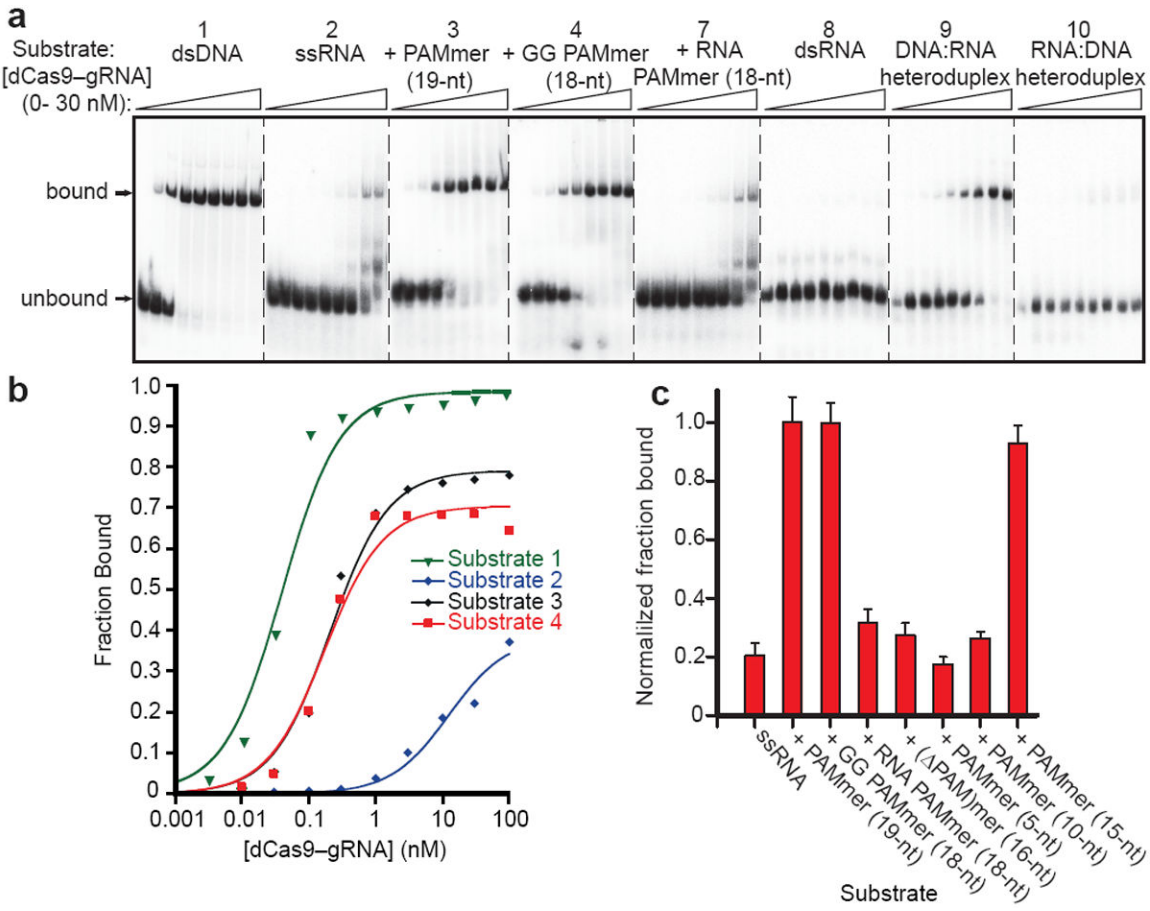

Figure 2. dCas9–gRNA binds ssRNA targets with high affinity in the presence of PAMmers

a, Representative electrophoretic mobility shift assay for binding reactions with dCas9–gRNA and a panel of 5′-radiolabeled nucleic acid substrates, numbered as in Fig. 1b. **b**, Quantified binding data for substrates 1–4 from (**a**) fit with standard binding isotherms. Measured dissociation constants from three independent experiments (mean ± s.d.) were 0.036 ± 0.003 nM (**1**), >100 nM (**2**), 0.20 ± 0.09 nM (**3**), and 0.18 ± 0.07 nM (**4**). **c**, Relative binding data for 1 nM dCas9–gRNA and 5'-radiolabeled ssRNA with a panel of different PAMmers. The data are normalized to the amount of binding observed at 1 nM dCas9–gRNA with a 19-nt PAMmer; error bars represent the standard deviation from three independent experiments.

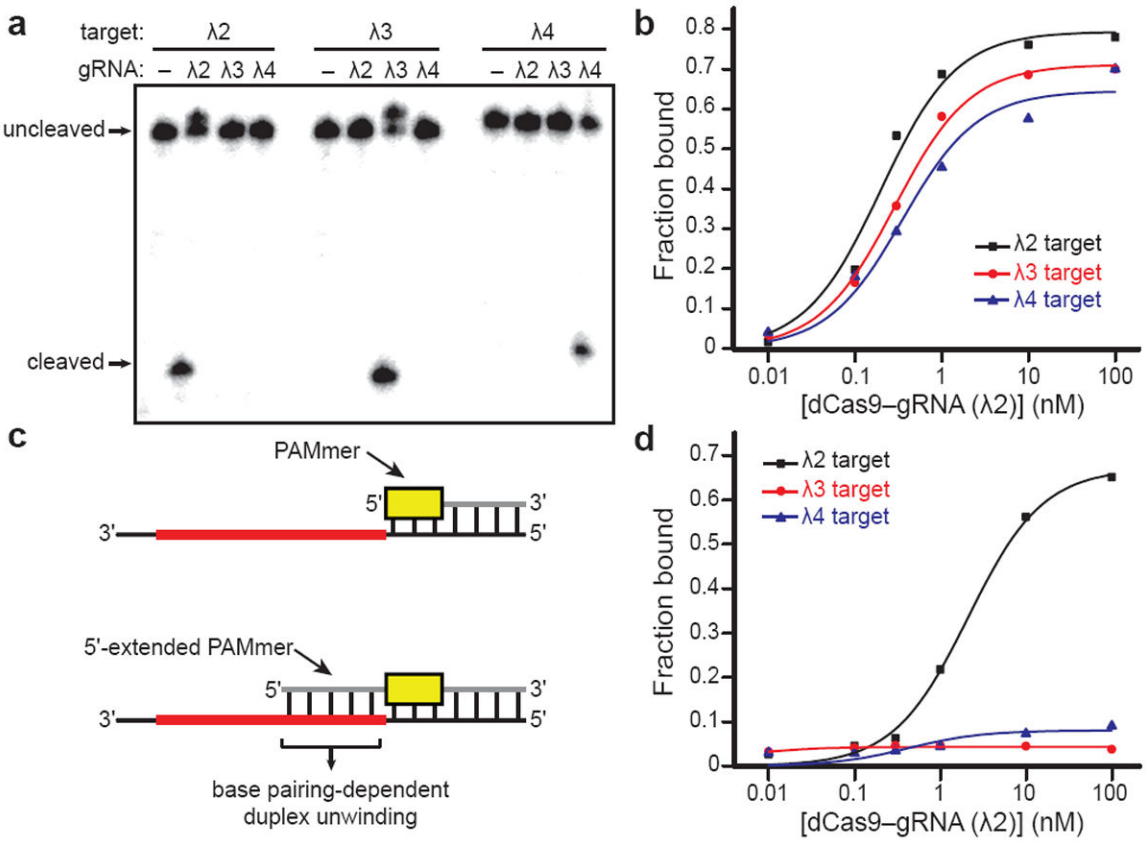

Figure 3. 5'-extended PAMmers are required for specific target ssRNA binding

a, Cas9 programmed with either λ2-, λ3-, or λ4-targeting gRNAs exhibits sequence-specific cleavage of 5'-radiolabeled λ2, λ3, and λ4 target ssRNAs, respectively, in the presence of cognate PAMmers. **b**, dCas9 programmed with a λ2-targeting gRNA exhibits similar binding affinity to λ2, λ3, and λ4 target ssRNAs in the presence of cognate PAMmers. Dissociation constants from three independent experiments (mean ± s.d.) were 0.20 ± 0.09 nM (**λ2**), 0.33 ± 0.14 nM (**λ3**), and 0.53 ± 0.21 nM (**λ4**). **c**, Schematic depicting the approach used to restore guide RNA-mediated ssRNA binding specificity, which involves 5'-extensions to the PAMmer that cover part of the target sequence. **d**, dCas9 programmed with a λ2-targeting gRNA specifically binds the λ2 ssRNA but not λ3 and λ4 ssRNAs in the presence of 5'-extended PAMmers. Dissociation constants from three independent experiments (mean ± s.d.) were 3.3 ± 1.2 nM (**λ2**) and >100 nM (**λ3** and **λ4**).

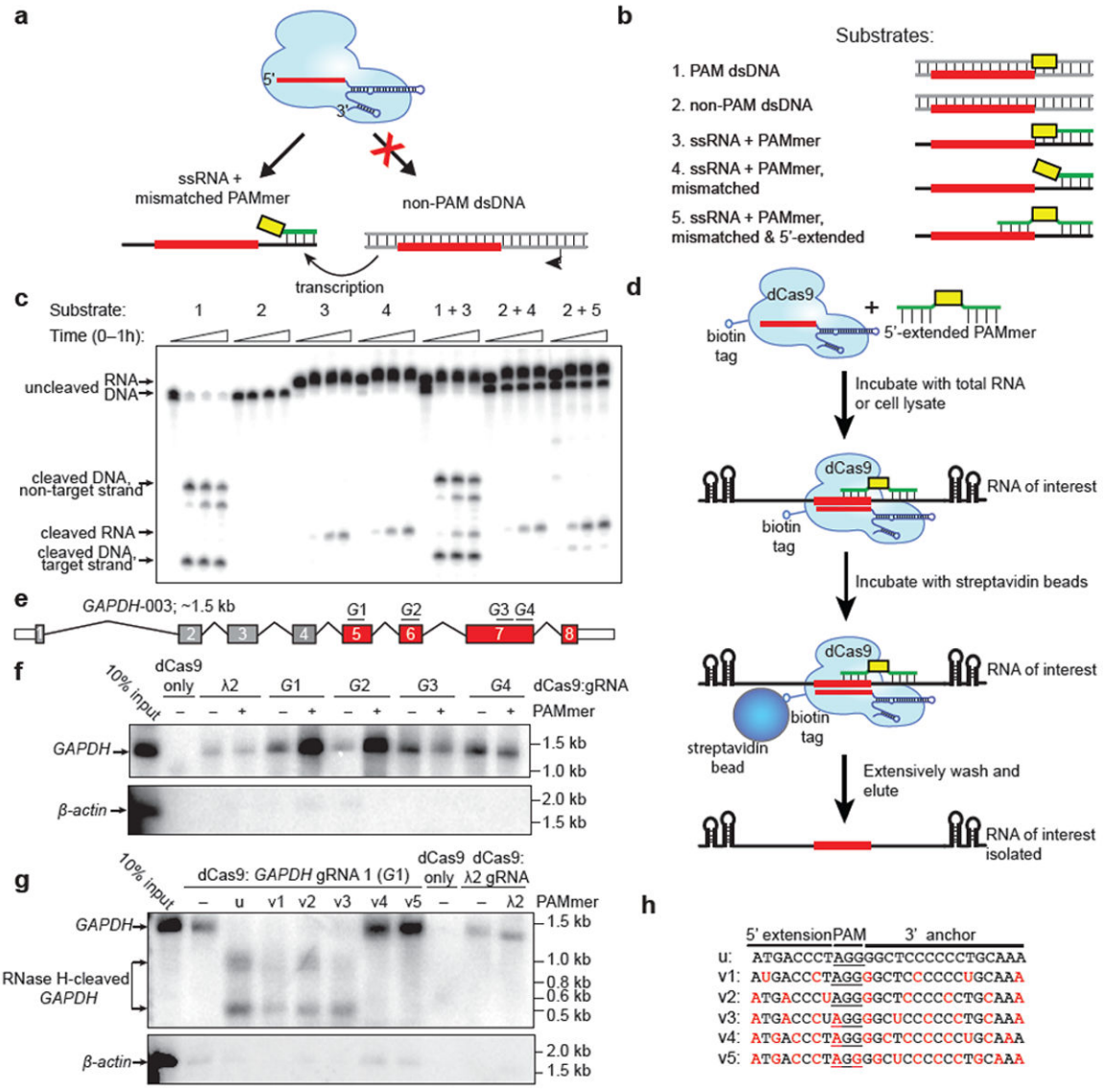

Figure 4. RNA-guided Cas9 can target non-PAM sites on ssRNA and isolate *GAPDH* mRNA from HeLa cells in a tagless manner

a,Schematic of the approach designed to avoid cleavage of template DNA by targeting non-PAM sites in the ssRNA target. **b**, The panel of nucleic acid substrates tested in (**c**). **c**, Cas9–gRNA cleaves ssRNA targets with equal efficiency when the 5'-NGG-3' of the PAMmer is mismatched with the ssRNA. This strategy enables selective cleavage of ssRNA in the presence of non-PAM target dsDNA. **d**, Schematic of the dCas9 RNA pull-down experiment. **e**, *GAPDH* mRNA transcript isoform 3 shown schematically, with exons common to all *GAPDH* protein-coding transcripts in red and gRNA/PAMmer targets *G*1-*G*4 indicated. **f**, Northern blot showing that gRNAs and 5'-extended PAMmers enable tagless isolation of *GAPDH* mRNA from HeLa total RNA; *β-actin* mRNA is shown as a control. **g**, Northern blot showing tagless isolation of *GAPDH* mRNA from HeLa cell lysate with varying 2'-OMe-modified PAMmers. RNase H cleavage is abrogated with v4 and v5

PAMmers; *β-actin* mRNA is shown as a control. **h**, Sequences of unmodified and modified *GAPDH* PAMmers used in **(g)**; 2'-OMe-modified nucleotides are shown in red.